DEPARTAMENTO DE BIOLOGÍA CELULAR Y ANATOMÍA PATOLÓGICA

FACULTAD DE MEDICINA

UNIVERSITAT DE BARCELONA

EL PAPEL DEL DIACILGLICEROL EN EL TRÁFICO DE MEMBRANAS EN LA ZONA ENTRE EL RETÍCULO ENDOPLASMÁTICO Y EL COMPLEJO DE GOLGI

Tesis presentada por Inés Fernández Ulibarri

para optar al título de Doctor por la Universidad de Barcelona

Anexo

Diacylglycerol Is Required for the Formation of COPI Vesicles in the Golgi-to-ER Transport Pathway◻ⱽ

Inés Fernández-Ulibarri,* Montserrat Vilella,* Francisco Lázaro-Diéguez,*†
Elisabet Sarri,* Susana E. Martínez,* Nuria Jiménez,‡ Enrique Claro,§
Isabel Mérida,‖ Koert N.J. Burger,¶ and Gustavo Egea*†

*Departament de Biologia Cellular i Anatomia Patològica, Facultat de Medicina and Institut d'Investigacions Biomèdiques August Pi i Sunyer, and †Institut de Nanociència i Nanotecnologia, Universitat de Barcelona, 08036 Barcelona, Spain; ‡Cellular Architecture and Dynamics and ¶Biochemical Physiology, Science Faculty and Institute of Biomembranes, Utrecht University, 3584 CH Utrecht, The Netherlands; and §Institut de Neurociències i Departament de Bioquímica i Biologia Molecular, Facultat de Medicina, Universitat Autònoma de Barcelona, 08193 Bellaterra, Barcelona, Spain; and ‖Departamento de Inmunología y Oncología, Instituto Nacional de Biotecnología, Universidad Autónoma de Madrid-Consejo Superior de Investigaciones Científicas, 28049 Madrid, Spain

Diacylglycerol is necessary for *trans*-Golgi network (TGN) to cell surface transport, but its functional relevance in the early secretory pathway is unclear. Although depletion of diacylglycerol did not affect ER-to-Golgi transport, it led to a redistribution of the KDEL receptor to the Golgi, indicating that Golgi-to-ER transport was perturbed. Electron microscopy revealed an accumulation of COPI-coated membrane profiles close to the Golgi cisternae. Electron tomography showed that the majority of these membrane profiles originate from coated buds, indicating a block in membrane fission. Under these conditions the Golgi-associated pool of ARFGAP1 was reduced, but there was no effect on the binding of coatomer or the membrane fission protein CtBP3/BARS to the Golgi. The addition of 1,2-dioctanoyl-*sn*-glycerol or the diacylglycerol analogue phorbol 12,13-dibutyrate reversed the effects of endogenous diacylglycerol depletion. Our findings implicate diacylglycerol in the retrograde transport of proteins from Golgi to the ER and suggest that it plays a critical role at a late stage of COPI vesicle formation.

INTRODUCTION

Recent observations from several laboratories indicate that membrane lipids regulate intracellular membrane transport, particularly in distal stages of the secretory pathway. Diacylglycerol (DAG) is a simple and small sized signal-transducing lipid which among other functions is necessary for protein transport from the Golgi complex to the cell surface both in yeast and in mammals. Thus, in budding yeast phosphatidylinositol (PI)-transfer Sec14p protein directly regulates DAG homeostasis in the Golgi complex and protein secretion (Bankaitis *et al.*, 1990; Kearns *et al.*, 1997; Huijbregts *et al.*, 2000). In mammals, the reduction of DAG levels at the Golgi caused by the depletion of Nir2 (a peripheral Golgi protein containing a PI-transfer domain) inhibits post-Golgi protein transport (Litvak *et al.*, 2005). DAG acts in the *trans*-Golgi network (TGN) as a membrane acceptor for specific proteins such as the protein kinase C (PKC) family member PKD/ PKCμ (Prestle *et al.*, 1996; Liljedahl *et al.*, 2001; Baron and Malhotra, 2002), and Hmun13 (Speight and Silverman, 2005).

PKD together with PKCθ, the trimeric G-protein subunits β/γ (Díaz Anel and Malhotra, 2005), and phosphatidylinositol-4 kinase IIIβ (Hausser *et al.*, 2005) directly participate in the post-Golgi transport of plasma membrane proteins containing basolateral sorting information (Yeaman *et al.*, 2004). On the other hand, Hmun13, through the recruitment of Rab34, participates in the Golgi-lysosome protein trafficking (Speight and Silverman, 2005). DAG also promotes the Golgi membrane targeting and activation of other C1 domain-containing signaling molecules such as other PKC isoforms (PKCη, PKCε, and PKCδ; Maissel *et al.*, 2006; Lehel *et al.*, 1995; Wang *et al.*, 1999, respectively) and Ras guanosine nucleotide-releasing proteins (RasGRPs; Caloca *et al.*, 2003), whose potential involvement in Golgi-associated transport functions remains unexplored.

The aforementioned Golgi-associated transport events linked to DAG levels can be envisioned in the framework of the DAG-phosphatidic acid (PA) interconversion. Thus, DAG is formed by phosphatidic acid phosphohydrolases (PAPs)—also known as lipid phosphate phosphatases (LPPs), and PA results from the activity of the DAG-consuming kinases (DAGKs). Although there are many DAGK isoforms, only DAGKα and DAGKδ have been localized to biosynthetic compartments such as the TGN (Alonso *et al.*, 2005) and the endoplasmic reticulum (ER; Nagaya *et al.*, 2002), respectively. To date only the PAP2b isoform has been located in the Golgi complex but in a cell-type–dependent manner (Sciorra and Morris, 1999). PA is formed by de novo synthesis from glyceraldehyde-3-phosphate or dihydroxyacetone-phosphate and acylCoAs and

also by breakdown of other phospholipids, in particular by the activity of phosphatidylcholine (PC)-specific phospholipase D enzymes (PLDs). Mammalian PLD1 (and PLD2, although this is controversial) is located in Golgi membranes (Freyberg *et al.*, 2001, 2002), supporting previous observations that indicated a direct role of PA in vesicle coat recruitment and budding (Siddhanta and Shields, 1998), as a result of ARF1-dependent enhancement of the PLD activity in the Golgi complex (Chen *et al.*, 1997). Therefore, PLD and PAP act in series to generate PA and DAG in (endo)membranes. Moreover, DAG is also generated through the action of sphingomyelin synthase (SMS), which is responsible for sphingomyelin (SM) and DAG formation (Ichikawa and Hirabayashi, 1998). In fact, one of the two SMS isoforms (SMS1) acts in the Golgi lumen (Huitema *et al.*, 2004). Another source of DAG in the Golgi are phosphoinositides. Thus, phosphatidylinositol-4-phosphate (PI,4P/PIP) or phosphatidylinositol 4,5-biphosphate (PI4,5P_2/PIP$_2$) is converted to DAG and inositol bis- or Tris-phosphate through phosphoinositide-specific phospholipase C (PI-PLC; Claro *et al.*, 1993; Rhee, 2001). In the plasma membrane and the Golgi apparatus, PLCε acts as a phosphoinositide-specific PLC (Satoh *et al.*, 2005). In the Golgi apparatus, the main phosphoinositide is PIP, which is actively generated by two phosphatidylinositol 4-kinases (PI4Ks) localized to the Golgi complex in mammalian cells (type III PI4Kβ and type II PI4Kα; Wang *et al.*, 2003; Weixel *et al.*, 2005). In contrast, PIP$_2$ at the Golgi is present at very low concentrations (De Matteis and Godi, 2004).

On the other hand, apart from functioning as a signaling molecule, the special biophysical properties of DAG may come into play (Leikin *et al.*, 1996; Goñi and Alonso, 1999). DAG has a small and electrically neutral polar head, explaining its pronounced cone shape and its capacity to undergo rapid transbilayer movement. DAG may induce membrane bending and facilitate the formation of highly curved membrane intermediates, thereby enhancing membrane constriction (Shemesh *et al.*, 2003) and fusion (Chernomordik *et al.*, 1995).

The potential coupling between the DAG-PA interconversion and CtBP3/BARS (BARS50) is of particular interest (Corda *et al.*, 2006) as this fission protein has recently been implicated in the biogenesis of COPI (coatomer)-coated (Yang *et al.*, 2005) and constitutive post-Golgi (Bonazzi *et al.*, 2005) transport carriers. BARS-dependent membrane fission requires long-chain acylCoAs and it was originally proposed to form PA by adding an acyl chain to lypophosphatidic acid (Weigert *et al.*, 1999; see also Gallop *et al.*, 2005). Alternatively, BARS may collaborate with lipid enzymes such as PLD, whose activity is required for numerous fission and membrane dynamics events (Tuscher *et al.*, 1997; Roth *et al.*, 1999; Freyberg *et al.*, 2003; Pathre *et al.*, 2003; Lee *et al.*, 2006). Like DAG, PA has special biophysical properties, and recent data indicate that PA could act as a docking site for interfacial insertion of positively charged membrane protein domains (Kooijman *et al.*, 2003, 2007), which with a PA-DAG interconversion cycle could be crucial for final membrane constriction/fission of coated/noncoated transport vesicles. In this respect, ARFGAP1 (ADP-ribosylating factor GTPase-activating protein) plays a central role in coupling cargo sorting and COPI vesicle formation on Golgi membranes by catalyzing GTP hydrolysis in the small G protein ARF1 (Lee *et al.*, 2005). ARFGAP1 constitutes a structural component of the COPI coat, and it contains a central motif named ALPS (ARFGAP1 lipid-packing sensor) that adsorbs preferentially onto highly curved membranes. This motif may allow the rate of GTP hydrolysis in ARF1 to be coupled with the membrane curvature induced by the COPI coat, which may lead to ARFGAP1 to function as a curvature sensor or inducer protein (Holthuis and Burger, 2003; Bigay *et al.*, 2005).

Although the molecular details of its Golgi targeting are unknown, a combination of interactions between transmembrane proteins and the COPI coat and lipids has been postulated (Antonny *et al.*, 1997; Bigay *et al.*, 2003; Mesmin *et al.*, 2007).

Here, we test the hypothesis that DAG regulates membrane trafficking at the ER–Golgi interface. We used a variety of pharmacological compounds that compromise cellular DAG production. Briefly, we found that the decrease of Golgi-associated DAG levels inhibits retrograde (Golgi-to-ER) but not anterograde (ER-to-Golgi) protein transport, reduces the ARFGAP1 pool in the Golgi complex and increases the amount of COPI-coated buds. These findings indicate that DAG participates in the fission of COPI transport carriers derived from early Golgi compartments.

MATERIALS AND METHODS

Reagents, Antibodies, and Plasmids

Brefeldin A (BFA), fumonisin B1 (FB1), *O*-tricyclo [5.2.1.0^{2,6}]dec-9-yl dithiocarbonate potassium salt (D609), 2-dioctanoyl-*sn*-glycerol (DOG), phorbol 12-myristate 13-acetate (PMA), phorbol 12,13-dibutyrate (PDBu), anti-VSV-G P5D4, anti-β-tubulin, anti-Flag monoclonal antibodies, and TRITC (tetramethylrhodamine isothiocyanate)-phalloidin were purchased from Sigma (St. Louis, MO). Latrunculin B, nocodazole, propanolol, U73122, and Mowiol were from Calbiochem (San Diego, CA). Rabbit polyclonal antibodies against the KDEL receptor (KDELr), galactosyltransferase (GalT), and mannosidase II (ManII) were kindly provided by the late H.-D. Söling (University of Göttingen), E. Berger (University of Zürich), and K. Moremen (University of Georgia, Athens), respectively. Mouse monoclonal antibodies to giantin, β-COP, and CTR433 were provided by H.-P. Hauri (Biozentrum, Basel), F. Wieland (University of Heidelberg) and M. Bornens (Institute Curie), respectively. mAb to BARS was both provided by A. Luini (Consorzio Mario Negri Sud [CMNS], Chieti, Italy) and purchased from BD Transduction Laboratories (San Diego, CA). Secondary antibodies conjugated to Cy3- or fluorescein isothiocyanate (FITC)-F(ab')$_2$ fragments were from Jackson InmunoResearch Laboratories (West Grove, PA). Plasmids encoding EGFP-C1b-PKCθ and EGFP-ARFGAP1 were from I. Merida (Consejo Superior de Investigaciones Científicas, Madrid) and H. Gad (CMNS, Chiety), respectively. Unless otherwise stated, all other chemicals were from Sigma.

Cell Lines and Cell Culture

COS-1, NRK, Vero, and HeLa cells, including stable HeLa cells that constitutively express YFP-GalT or GST-Flag-PKD-KD (a gift of V. Malhotra, University of California, San Diego, CA), were cultured in DMEM (Invitrogen, Paisley, United Kingdom) containing 10–20% of fetal calf serum (FCS; GIBCO/BRL Invitrogen, Paisley, United Kingdom). HeLa spinner cells were cultured in RPMI 1640 (Biochrom, Berlin, Germany) containing 7.5% FCS. All culture media were supplemented with sodium pyruvate (1 mM), glutamine (2 mM), penicillin (100 U/ml), and streptomycin (100 μg/ml). Cells were grown in a humidified incubator in 5% CO$_2$ at 37°C.

Isolation of Golgi Membranes

Golgi fractions from HeLa cells were prepared at 4°C following a modification of the method established by Balch *et al.* (1984). Hela spinner cells were grown in suspension, and they reached a 5×10^8 cells were treated either with propanolol or U73122. They were harvested by centrifugation (10 min at 500 $\times$ *g*), washed twice with PBS (10 min at 500 $\times$ *g*), twice with homogenization buffer (250 mM sucrose in 10 mM Tris-HCl, pH 7.4; 10 min at 1,500 $\times$ *g*), resuspended in four volumes of homogenization buffer. Thereafter, cells were homogenized using the Ball-Balch homogenizer device. The homogenate was brought to a sucrose concentration of 37% (wt/wt) by the addition of 62% (wt/wt) sucrose in 10 mM Tris-HCl, pH 7.4, and EDTA (1 mM, final concentration). Twelve milliliters of this solution was placed at the bottom of a SW 28 tube and carefully overlaid with 15 ml of sucrose at 35% (wt/wt) and 9 ml sucrose at 29% (wt/wt) in 10 mM Tris-HCl (pH 7.4). Gradients were centrifuged at 25,000 rpm for 2.5 h. Golgi-enriched membrane fraction were recovered at the 35–29% sucrose interphase and subsequently frozen in aliquots in liquid nitrogen and stored at −80°C. Protein concentration was determined using the Bradford assay.

Diacylglycerol Content

Golgi membrane lipids from control and propanolol- or U73122-treated cells were extracted in glass tubes with chloroform/methanol/HCl (Bligh and Dyer, 1959). To determine diacylglycerol content in these lipid extracts, quantitative conversion to [^{32}P]phosphatidic acid by diacylglycerol kinase was performed as described (Preiss *et al.*, 1987). Chloroform extracts (850 μl) of isolated Golgi membranes (70 μg) or 1-stearoyl-2-arachidonoyl-*sn*-glycerol

I. Fernández-Ulibarri *et al.*

(Sigma) samples (30–500 pmol) were evaporated under a gentle stream of nitrogen, and the dried lipids were solubilized in 20 μl of 7.5% octyl-β-D-glucoside, 5 mM cardiolipin, and 1 mM diethylenetriaminepentaacetic acid (DETAPAC) by sonication in a bath (50–60 Hz) for 30 s, after incubation for 10 min at room temperature. To this lipid solution, we added 50 μl of 100 mM imidazole/HCl buffer, pH 6.6, containing 100 mM NaCl, 25 mM MgCl$_2$, and 2 mM EGTA, and then 10 μl of fresh 20 mM dithiothreitol (DTT) in 1 mM DETAPAC, pH 7.0, and 10 μl of a diacylglycerol kinase (Calbiochem) solution (0.25 mg/ml) in 20 mM imidazole/HCl buffer, pH 6.6, containing 2 mM DETAPAC. The reaction was started by adding 10 μl of 100 mM imidazole/HCl buffer, pH 6.6, containing 1 mM DETAPAC, 10 mM ATP, and 0.6 μCi [γ-^{32}P]ATP (Amersham Pharmacia Biotech, Piscataway, NJ, 3 Ci/mmol, 2 mCi/ml), and was carried out for 30 min at room temperature. Reactions were stopped with 0.6 ml of chloroform/methanol/10 M HCl (100:200:1 by vol), followed by addition of 0.25 ml each of water and chloroform, in order to split two phases. The lower (chloroform) phases were washed with chloroform-saturated methanol/water (1:1), evaporated under nitrogen, dissolved in 20 μl of chloroform/methanol (4:1), and developed on silica gel 60 thin-layer chromatography (TLC) plates using chloroform/methanol/acetic-acid/water (100:60:16:8; vol/vol/vol/vol) and air-dried. [^{32}P]Phosphatidic acid was quantified using PhosphorImager (Molecular Dynamics, Sunnyvale, CA) and NIH Image software.

Transient Transfections

Cells were grown to 70–80% confluence and then transfected either with EGFP-C1b-PKCθ or GFP-ARFGAP1 using the Effectene transfection method (Qiagen, Valencia, CA) according to the manufacturer's instructions. Unless otherwise indicated, experiments were carried out 12–16 h after transfection. Cells expressing EGFP-C1b-PKCθ or GFP-ARFGAP1 for confocal microscopy were treated with cycloheximide (100 μg/ml) 60 min before the assay.

VSV-G Infection and VSV-G Transport Assay

Experiments were carried out as previously indicated (Valderrama *et al.*, 1998).

Immunofluorescence and Quantitative Image Analysis

Indirect immunofluorescence assays were carried out using the following antibody dilutions: anti-KDELr, 1:1000; anti-Gal-T, 1:100; anti-giantin, 1:500; anti-ManII, 1:1000; anti-β-COP 1:1000; anti-β-tubulin, 1:50; anti-BARS, 1:50; anti-VSV-G, 1:50; anti-Flag, 1:100; anti-CTR433, 1:5; Cy3-anti-mouse, 1:50; anti-mouse-FITC, 1:100; and anti-rabbit-Cy3– and anti-rabbit-FITC–conjugated secondary antibodies, 1:250. Immunostained coverslips were mounted on microscope slides using Mowiol. Microscopy and imaging were performed either with an Olympus BX60 epifluorescence microscope equipped with a cooled Olympus CCD camera (Lake Success, NY) or with a Leica TCS-NT confocal microscope (Heerbrugg, Switzerland). The images were processed using Image J software. To quantify cytoplasmic fluorescent punctuate structures containing KDELr, eight-bit gray scale nonsaturated images were set at an arbitrary threshold value of 90. For each cell, the number of stained structures (defined as being smaller than 600 pixels) over threshold was scored covering the total cytoplasmic area.

Time-Lapse Fluorescence Confocal Microscopy

Time-lapse fluorescence confocal microscopy experiments were carried out using a Leica TCS SL laser-scanning confocal spectral microscope (Leica Microsystems Heidelberg, Manheim, Germany) with Argon and HeNe lasers attached to a Leica DMIRE2 inverted microscope equipped with an incubation system with temperature and CO$_2$ control. For visualization of GFP, images were acquired using a PL APO 63× oil immersion objective lens (NA 1.32), 488-nm laser line, excitation beam splitter RSP 500, and an emission range detection: 500–610 nm and the confocal pinhole set at 4.94 Airy units. Images were acquired at 30-s intervals for 1–2 h, and optical sectioning was necessary to capture the whole signal. The excitation intensity was attenuated to 5% of the half-laser power to avoid significant photobleaching. Image treatment and movie assembly were performed using the Image Processing Leica Confocal Software. PMA (250 nM) was added to DMEM after the first frame, and images were recorded every 15 s. Then, after the forty-first frame, DOG (3 μM) or PDBu (250 nM) was mixed with PMA. Propranolol (60 μM) and DOG (3 μM) were added to DMEM after the first frame. Cells were preincubated with DOG (3 μM, 15 min) and then mixed with propanolol, and images were recorded every 15 s. BFA (5 μg/ml), propanolol (60 μM), or BFA together with propanolol was added to the DMEM in the same conditions, but in this case images were recorded every 10 s. Films and time series of fluorescent images taken from films were processed using Image J software.

Electron Microscopy, Electron Tomography, and 3D Modeling

For transmission electron microscopy (TEM), Vero, NRK, and HeLa cells were rapidly fixed with 1.25% glutaraldehyde in PIPES buffer (0.1 M, pH 7.4) containing sucrose (2%) and Mg$_2$SO$_4$ (2 mM) for 60 min at 37°C. Cells were then gently scraped, pelleted at 100 × *g* for 10 min, rinsed in PIPES buffer (3 ×

5 min), and postfixed with 1% (wt/vol) OsO$_4$, 1% (wt/vol) K$_3$Fe(CN)$_6$ in PIPES buffer for 1 h at room temperature in the dark. Cells were then treated for 5 min with tannic acid (0.1%) in PIPES buffer, rinsed in distilled water, block-stained with 1% uranyl acetate in 70% ethanol for 1 h, dehydrated and graded ethanol solutions, and finally embedded in Epon plastic resin (EMS, Hatfield, PA). Ultrathin sections (50–70-nm thick) were stained with lead citrate and observed on a JEOL 1010 electron microscope (Peabody, MA). Micrographs of randomly selected areas were obtained with a Gatan Bioscan digital camera (Pleasanton, CA) at the same final magnification (50,000×) and analyzed using point-counting procedures. The stereological parameters were determined using standard procedures. The minimum sample size of each stereological parameter was determined by the progressive mean technique (confidence limit of 5%). The results were expressed as means ± SD and compared using Student's *t* test.

For electron tomography and 3D modeling, sections (250 nm) of chemically fixed, Epon-embedded NRK cells were transferred to Butvar-coated copper slot grids. Colloidal gold particles (10 nm) were added to one side of the grid as markers to align the series of tilted images. Tilt series of representative Golgi stacks were automatically recorded (Ziese *et al.*, 2002) at 200 kV using a Tecnai20 electron microscope (FEI/Philips Electron Optics, Eindhoven, The Netherlands) equipped with a slow-scan CCD camera (TemCam F214, TVIPS [Tietz Video and Image Processing Systems], Gauting, Germany) and a motorized goniometer. Recording was made with Xplore 3D software package; FEI) at a final magnification of 14,000×. Every specimen was tilted about two orthogonal axes from −65° to +65° at 1° intervals, resulting in two datasets of 131 high-resolution digital images. Images were then aligned using the program package IMOD (Kremer *et al.*, 1996), and a tomogram was computed from each tilt series. The two single-axis tomograms were merged into one (Mastronade, 1997), and the tomographic dual-axis reconstruction was interpreted and modeled using IMOD software.

Statistical Analysis

For statistical computation and estimation of significance, we used the online software GraphPad (San Diego, CA; www.graphpad.com). Control and differently treated cells were run through unpaired ANOVA and, when appropriate, Student's *t* test.

RESULTS

Both Propanolol and U73122 Reduced DAG Levels in the Golgi Complex

To study the role of DAG in protein transport at the ER–Golgi interface, we examined a range of pharmacological agents (Figure 1) that had been reported to decrease DAG levels in a wide variety of cell types. These compounds are as follows: 1) propanolol, which inhibits PAP and therefore prevents dephosphorylation of PA to DAG (Pappu and Hauser, 1983; Roberts *et al.*, 1998; Baron and Malhotra, 2002); 2) D609, which inhibits PC-specific PLC (Schutze *et al.*, 1992; Exton, 1994) and SMS1 (Luberto and Hannun, 1998); 3) U73122, which inhibits PI-PLC (Bleasdale *et al.*, 1990; Thompson *et al.*, 1991; Jun *et al.*, 2004); and 4) FB1, which inhibits ceramide synthase and thus deprives SM synthase of substrate and lowers DAG (Wang *et al.*, 1991; Wu *et al.*, 1995; Merrill *et al.*, 2001). First, we examined whether these compounds perturb the organization and dynamics of microtubular and actin cytoskeletons, because an efficient ER–Golgi interface membrane trafficking is dependent on the integrity of both cytoskeletons (Murshid and Presley, 2004; Egea *et al.*, 2006). NRK and Vero cells treated with propanolol (60 μM/30 min), U73122 (6 μM/30 min), D609 (500 μM/30 min), or FB1 (25 μg·ml^{-1}/24 h) showed microtubule and actin cytoskeleton organization (Supplementary Figure 1A) and dynamics (Supplementary Figure 1, B and C) that was indistinguishable from control. However, D609 blocked the reconstitution of microtubules (Supplementary Figure 1B) and actin filaments (unpublished data) that was expected after the respective removal of nocodazole and latrunculin B. Consequently, we ruled out the use of D609.

We then examined the effects of propanolol, U73122, and FB1 on the DAG pool in the Golgi complex. We used the concentrations stated above, so that the cytoskeleton would not be compromised. We used 1) the inactive mutant form of PKD (PKD-K618N/PKD-KD), 2) a biochemical assay to
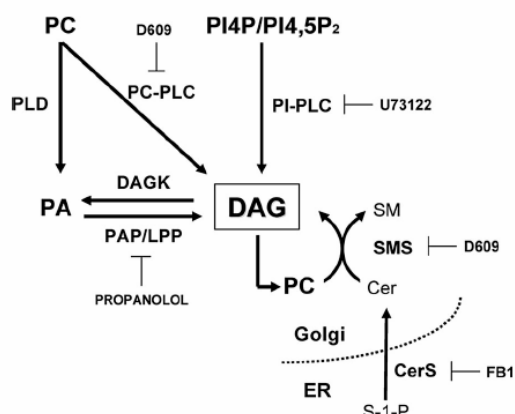
Figure 1. Signaling pathways that are most likely to be implicated in the generation of DAG at the Golgi. Enzymes involved in the production of DAG and the inhibitors used in this study are shown. DAG degradation enzymes and the metabolites generated from this lipid are omitted for simplicity. Cer, ceramide; CerS, CoA-dependent dihydroceramide/ceramide synthase; DAG, diacylglycerol; DAGK, dicylglycerol kinase; FB1, fumonisin B1; PA, phosphatidic acid; PAP/LPP, phosphatidic acid phosphatase/lipid phosphate phosphatase; PC, phospatidylcholine; PI4P, phosphatidylinositol, 4 monophosphate; $PI4,5P_2$, phosphatidylinositol 4,5-biphosphate; PC-PLC, phosphatidylcholine-specific phospholipase C; PI-PLC, phosphoinositides-specific phospholipase C; PLD, phospholipase D; SM, sphingomyelin; SMS, sphingomyelin synthase 1; S-1-P, sphingosine-1-phosphate.

measure DAG levels in Golgi fractions isolated from treated cells, and/or 3) the DAG-dependence localization of the C1 domain of PKCθ in the Golgi (see below). With respect to the former approach, it is known that DAG is sufficient and necessary for the recruitment of PKD to TGN membranes (Maeda *et al.*, 2001). Thus, the HeLa stable cell line expressing GST-flag-PKD-KD was treated with propanolol, U73122, or FB1. After 15 min of treatment with propanolol (Figure 2, C and D), U73122 (Figure 2, G and H), or FB1 (unpublished data; see Baron and Malhotra, 2002), PKD-KD was redistributed from the Golgi to the cytoplasm. Moreover, PKD-KD returned to the Golgi when propanolol (Figure 2, E and F), U73122, or FB1 (unpublished data) was washed out. We also measured DAG in Golgi membranes isolated from HeLa cells treated with propanolol or U73122. Both propanolol and U73122 decreased DAG levels to ~45% of control values (Figure 2I). In addition, FB1 (as well as propanolol and U73122) induced the complete redistribution of the GFP-C1b domain of PKCθ from the Golgi to the cytoplasm (Supplementary Figure 3B and see below). This is indicative of a robust decrease of the DAG pool in the Golgi caused by FB1 treatment. Therefore, propanolol, U73122, and FB1 diminished Golgi-associated DAG levels without altering the organization and dynamics of actin or microtubular cytoskeleton. This validates their use in examining the potential involvement of DAG in membrane trafficking at the ER–Golgi interface.

Propanolol and U73122 Blocked the Retrograde But Not Anterograde Membrane Transport

To assess whether the maintenance of DAG levels in the Golgi is required for ER–Golgi interface membrane trafficking, we examined the ER-to-Golgi transport of VSV-G protein. Cells were infected with the ts045 VSV mutant, which
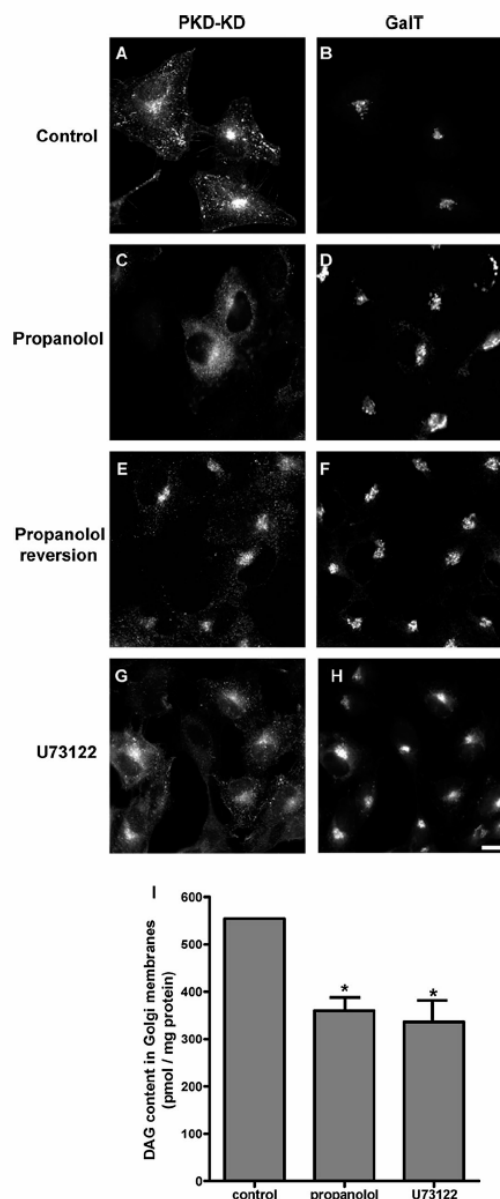

Figure 2. Treatment with propranolol or U73122 decrease DAG levels in the Golgi. HeLa cells that stably express GST-flag-PKD-KD (K618N) were treated with propranolol (60 μM/15 min; C and D) or U73122 (6 μM/15 min; G and H). Thereafter, cells were coimmunostained with a mAb anti-flag to visualize PKD-KD (A, C, E, and G) and a polyclonal antibody to galactosyltransferase (GalT) to visualize the Golgi complex (B, D, F, and H). Note that the treatment with propranolol (C) or U73122 (G) induced the redistribution of PKD-KD from the Golgi (A) to the cytosol (C and G). When propranolol was removed from the culture medium (45 min), the PKD-KD redistributed in the cytosol was returned to the Golgi (E and F). (I) DAG content of isolated Golgi membranes from untreated (control), propranolol (60 μM/15 min)-, or U73122 (6 μM/15 min)-treated HeLa cells measured by the DAG-kinase assay. Statistical significance, *$p \leq 0.05$. Bar, 10 μm.

I. Fernández-Ulibarri *et al.*

at nonpermissive temperature (40°C) was retained at the ER (Supplementary Figure 2A). When cells were transferred to permissive temperature (32°C), VSV-G was transported to the plasma membrane (Supplementary Figure 2C) crossing the Golgi complex (Supplementary Figure 2B). When VSV-infected cells were treated with propanolol, U73122, or FB1, VSV-G transport from the ER to the Golgi was unaltered (Supplementary Figure 2, E, H, and K, respectively). In accordance with these results, neither propanolol nor U73122 (unpublished data) nor FB1 (Supplementary Figure 3) affected the normal reassembly of the Golgi in BFA washed-out cells. Interestingly, the VSV-G post-Golgi transport to the plasma membrane was blocked only in propanolol- and FB1-treated cells (Supplementary Figure 2, F and L, respectively) but not in those cells treated with U73122 (Supplementary Figure 2I).

Next, we examined the effect of low DAG in the Golgi on Golgi-to-ER transport. When propanolol, U7312,2 or FB1 was added subsequently to BFA, the Golgi disassembly occurred normally (unpublished data). Conversely, when BFA was added either at the same time as, or just after, the pretreatment with propanolol or U73122, the redistribution of Golgi markers (Figure 3, A–D) to the ER was blocked. Strikingly, FB1 had no effect on the normal Golgi disassembly produced by BFA (Supplementary Figure 3A). Thus, unlike FB1, propanolol and U73122 perturb the Golgi-to-ER membrane flow. To confirm this result in a more physiological setting, we examined the subcellular distribution of the KDELr. KDELr mediates the return to the ER of ER-resident proteins that have escaped to the Golgi. At steady state, KDELr was observed both in the Golgi and in numerous punctate cytoplasmic structures, which represent tubulove-

sicular structures that are continuously cycling between the ER and the Golgi (Figure 3E). Any modification of this distribution reflects an alteration in the retrograde or anterograde traffic rates (Lewis and Pelham, 1992). In Vero cells treated with propanolol (Figure 3F) or U73122 (Figure 3G), KDELr staining was reduced in cytoplasmic fluorescent punctate structures (Figure 3H). Similar morphological features were also observed in NRK and HeLa cells (unpublished data). Moreover, morphological alterations were more robust in propanolol-treated than in U73122-treated cells (compare quantitative analysis shown in Figures 3, D and H). Cells treated with FB1 did not show any alteration in the subcellular distribution of KDELr (unpublished data). Taken together, our results indicate that only DAG pool(s) altered by propanolol and U73122 seem to be required for retrograde (Golgi-to-ER) but not for anterograde (ER-to-Golgi) membrane trafficking.

It has been postulated that the inhibition by propanolol of PAP/LPP and the inhibition by U73122 of PI-PLC may reduce different molecular species of DAG (Carrasco and Mérida, 2004). Therefore, we examined whether propanolol or U73122 have an additive or synergic effect on the Golgi-to-ER protein transport. Cells were treated with lower concentrations of propanolol and U73122 that do not alter BFA-induced Golgi disassembly (unpublished data) or the subcellular distribution of KDELr (Supplementary Figures 5, A and B). When propanolol and U73122 were added together there was an inhibition of the BFA-induced Golgi-to-ER membrane backflow (unpublished data) and a change in the subcellular distribution of the KDELr (Supplementary Figure 4C). These findings were indistinguishable from those observed for each compound used separately at higher
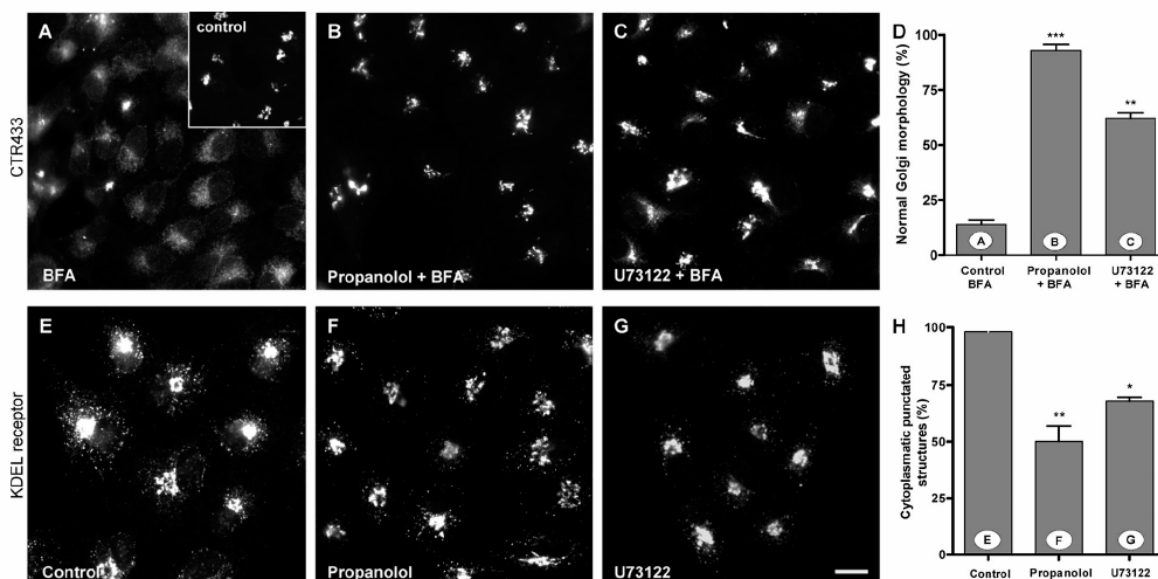

Figure 3. Propanolol and U73122 block the BFA-induced Golgi disassembly and alter the steady-state staining pattern of the KDEL receptor. (A–D) Vero cells were treated with BFA (5 μg/ml for 20 min) alone (A), with propanolol (60 μM) plus BFA (propanolol was added 5 min before BFA; B), or U73122 (6 μM) plus BFA (U73122 was added 5 min before BFA; C). Cells were then processed for immunofluorescence microscopy using monoclonal anti-CTR433 to visualize the Golgi complex (see inset in A for control cells). Both propanolol (B) and U73122 (C) blocked the BFA-induced disassembly of the Golgi complex (A). Quantitative analysis of these results is shown in D. (E–H) The steady-state subcellular distribution of KDEL receptor (KDELr) using anti-KDELr polyclonal antibodies was also examined in control and propanolol (60 μM/60 min; F) or U73122 (6 μM/60 min; G)-treated Vero cells. Both propanolol and U73122 treatments induced a significant change in the steady-state staining pattern of the KDELr: the fluorescent cytoplasmic KDELr-containing punctate structures are no longer seen. These observations were quantified, as shown in H. Statistical significance, **$p \leq 0.01$ and ***$p \leq 0.001$. Bar, 10 μm.

concentrations (Figure 3, F and G). Next, when cells were coincubated with the usual working concentrations of propanolol (60 μM) plus U73122 (6 μM), the change in the subcellular distribution of KDELr lasted longer than when the two agents were used separately (120 vs. 60 min). Similarly, coincubation resulted in a more persistent inhibition of BFA-induced Golgi (60 vs. 30 min). Overall, these results indicate that different pools of DAG participate in Golgi-to-ER membrane trafficking.

Propanolol and U73122 Perturbed the BFA-induced Formation of Tubules from Golgi Membranes

Next, we analyzed whether the inhibition of the BFA-mediated redistribution of Golgi membranes to the ER by propanolol and U73122 is the result of the inhibition of BFA-induced coatomer dissociation. We examined the kinetics of dissociation of coatomer from Golgi membranes in the presence of BFA using anti-β-COP antibodies (Supplementary Figure 5). Propanolol or U73122 added just before or at the same time as BFA did not inhibit the BFA-induced dissociation of coatomer from Golgi membranes (Supplementary Figure 5, H and K). The distribution of β-COP was affected neither by propanolol nor U73122 (Supplementary Figure 5, C and E). After the dissociation of coatomer and ARF1 from Golgi membranes (Klausner *et al.*, 1992), BFA promotes the formation of Golgi-derived tubules that finally fuse to the ER. Next we examined whether propanolol and U73122 impair the Golgi tubulation induced by BFA. We used time-lapse images of Hela cells expressing YFP-tagged GalTase recorded during the treatment with propanolol or U73122 plus BFA (Figure 4). As expected (Sciaky *et al.*, 1997), cells treated with BFA alone showed numerous thin Golgi-derived tubules, which after a few minutes irreversibly fused with the ER, leading to the disappearance of Golgi fluorescence (Figure 4A; Supplementary Video 1). Propanolol not only reduced the density of BFA-induced tubules emerging from the Golgi but also increased their diameter (compare Figure 4A, panel 7′ with 4B, panel 10′, arrow; also compare Supplementary Video 1 with Supplementary Video 2). Moreover, the few thick tubules produced by BFA in the presence of propanolol grew in length but failed to fuse with the ER, with most returning to the Golgi (white arrow in Figure 4B; Supplementary Video 2). U73122-treated cells

also showed a significant slowing-down of the BFA-induced Golgi tubulation process but tubules were similar to those seen after BFA treatment alone. As observed in propanolol-treated cells, they also remained in the cytoplasm for longer (unpublished data). Hence, the decelerated Golgi disassembly induced by BFA in propanolol- or U73122-treated cells was not caused by an alteration in the kinetics of coatomer dissociation from Golgi membranes. Rather, both agents interfered with the formation and the progress of Golgi-derived tubules and/or their subsequent fusion with the ER.

DOG and PDBu prevented the Propanolol/U73122-induced Inhibition of Retrograde Transport of KDELr

To establish a direct link between the effects of propanolol or U73122 on ER–Golgi interface membrane trafficking and the decrease of DAG pool in the Golgi, we examined whether these trafficking alterations would be prevented by the exogenous resupplementation of the DAG pool. We used short acyl chain DOG and the DAG analogue PDBu. Control experiments demonstrated that neither DOG (3 μM) nor PDBu (250 nM) altered the actin or microtubule cytoskeleton (unpublished data). We next checked that DOG and PDBu are indeed incorporated into Golgi membranes. We took advantage of the fact that DAG pools are recognized by proteins that contain a conserved sequence of 50 amino acids, the so-called C1 domain (Colón-González and Kazanietz, 2006). This is the case of PKCθ, whose C1b domain behaves as a sensor of DAG (Quest *et al.*, 1994). When cells were transfected with the GFP-C1 domain and treated with phorbol myristate acetate (PMA, a hydrophobic DAG analogue that it is preponderantly incorporated into the plasma membrane), the GFP-C1 domain in the Golgi (Figure 5, B and E) was reduced (Figure 5A), because it was quickly redistributed to the plasma membrane (Figure 5, C and F; Supplementary Video 3) as previously reported in other cell types (Carrasco and Merida, 2004). Less than 20% of Golgi-associated GFP-C1b domain fluorescence in PMA-treated cells remained at the Golgi after 5–10 min of PMA treatment (Figure 5A). At longer times, the fluorescence rose very slowly (Figure 5A; Supplementary Video 3). On this basis, we added DOG or PDBU at the moment at which the Golgi-associated GFP-C1b fluorescence was the lowest (between 5 and 10 min after PMA treatment). We expected to see a
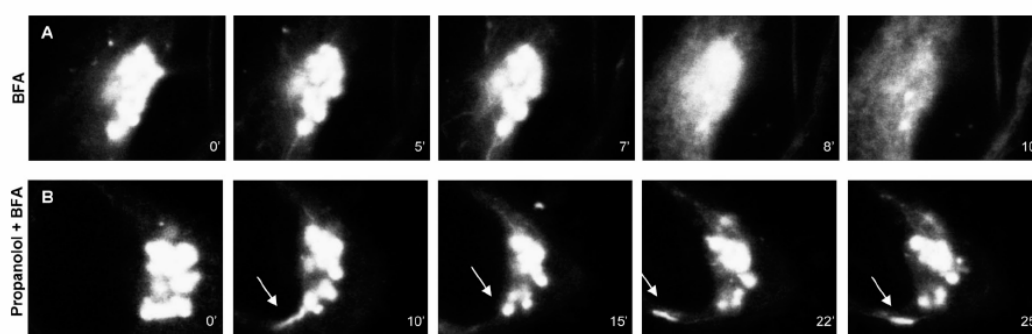

Figure 4. Propanolol impairs both the formation of normal BFA-induced Golgi-derived tubules and their subsequent fusion to the ER. Time series of fluorescent images taken from films of HeLa cells constitutively expressing YFP-GalTase during the Golgi disassembly induced by BFA (5 μg/ml; A) or propanolol (60 μM) plus BFA (B). BFA induced the formation of thin YFP-GalTase–containing tubules emerging from the Golgi (5- and 7-min frames). Subsequently, tubules fused with the ER, giving rise to the characteristic ER-like staining pattern (10-min frame). In contrast, propanolol pretreatment prevented BFA-induced Golgi disassembly (B). After 25 min of propanolol plus BFA treatment, the Golgi was still clearly visible (B) and a representative large, thick tubule emerging from the bottom of the Golgi was seen to grow and then retract into the Golgi. Videos corresponding to frames shown in A were obtained from Supplementary Video 1 (YFP-GalTase HeLa cells plus BFA) and those shown in B were from Supplementary Video 2 (YFP-GalTase HeLa cells propanolol plus BFA).
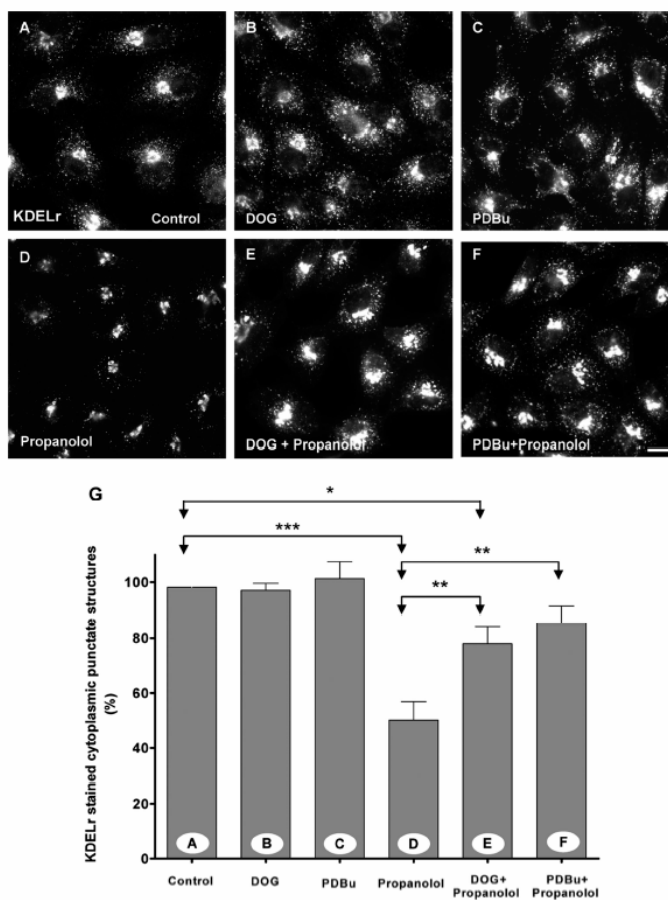
DAG and the ER–Golgi Membrane Trafficking

Figure 7. DOG and PDBu prevent the propanolol-induced alteration of the subcellular distribution of the KDELr. Vero cells were treated for 1 h with DOG (3 μM; B), PDBu (250 nM; C), propanolol (60 μM; D), DOG plus propanolol (E), or PDBu plus propanolol (F). Thereafter, cells were fixed and stained for KDELr. As shown in Figure 3, at steady state, the KDELr was located in the Golgi and in numerous punctated cytoplasmic structures (A). This staining pattern was not altered by DOG (B) or PDBu (C) treatments. Propanolol decreased the fluorescent punctate cytoplasmic structures, revealing a more Golgi-like staining pattern (D). When DOG (E) or PDBU (F) was added with propanolol, the resulting subcellular distribution of the KDELr was practically indistinguishable from control (A). (G) Quantitative analysis of the percentage of fluorescent punctate cytoplasmic structures in each experimental condition (A–F). Statistical significance, *$p \leq 0.05$, **$p \leq 0.01$, and ***$p \leq 0.001$. Bar, 10 μm.

tested whether DOG or PDBu prevented the alterations caused by propanolol (Figure 7) or U73122 (unpublished data) in the retrograde protein trafficking. Cells were simultaneously incubated with DOG or PDBu plus propanolol or U73122, and the subcellular distribution of KDELr was examined. As shown in Figure 7, the staining pattern of KDELr in DOG or PDBu plus propanolol-treated cells was apparently indistinguishable from control (compare Figure 7, E and F, with 7A). Neither DOG nor PDBu alone altered the KDELr distribution (Figure 7, B and C). DOG (Supplementary Figure 6) and PDBu (unpublished data) also significantly counteracted the inhibition of BFA-induced Golgi disassembly in propanolol- or U73122-treated cells. Overall, our results show that exogenously added DAG efficiently compensates for the decrease in endogenous DAG in the Golgi and prevents the alterations in Golgi-to-ER membrane traffic induced by propanolol and U73122.

DOG and PDBu Prevented Cisternae Swelling and the Abnormally High Density of Golgi-associated Buds Produced by Propanolol and U73122

We examined the ultrastructure of the Golgi complex in Vero (Figure 8), NRK (Figure 9), and HeLa (unpublished data) cells treated with propanolol and U73122 despite that by immunofluorescence the Golgi complex remained apparently unaltered (Figure 2). Conventional TEM analysis indi-

cates that propanolol (Figures 8B and 9B) and U73122 (Figure 8C) both induce fragmentation of Golgi cisternae, whereas propanolol treatment also results in cisternal swelling. Notably, both agents gave rise to numerous coated membranes in close vicinity of Golgi cisternae, which, judged by their ultrastructure and localization, carried a COPI coat (Figures 8B and 9B, propanolol, arrowheads and insets; Figure 8C, U73122, arrowheads; Table 1). In control cells, these Golgi-associated circular profiles were almost undetectable (Figures 8A and 9A; Table 1). In conventional TEM analysis of ultrathin (50–70 nm) sections, circular membrane profiles cannot be assigned unequivocally to free transport carriers (vesicles) because they might also correspond to cross-sectioned membrane tubules or buds. However, such an analysis is possible using thicker sections (~250 nm) and electron tomography. Tomograms of propanolol-treated cells (Supplementary Video 7) clearly indicated that cisternae were swollen and carried an abnormally high number of membrane buds attached to the cisterna through a narrow neck (see contoured structures in Figure 9C). 3D models of these tomograms confirmed the presence of numerous nascent transport carriers that appeared to be arrested before membrane fission (vesicles colored in red in Figure 9D, 1–3; Supplementary Video 8) and that carried a characteristic electron-dense fuzzy COPI coat (Figures 8B and 9B, arrowheads and insets, and 9C; Supplementary
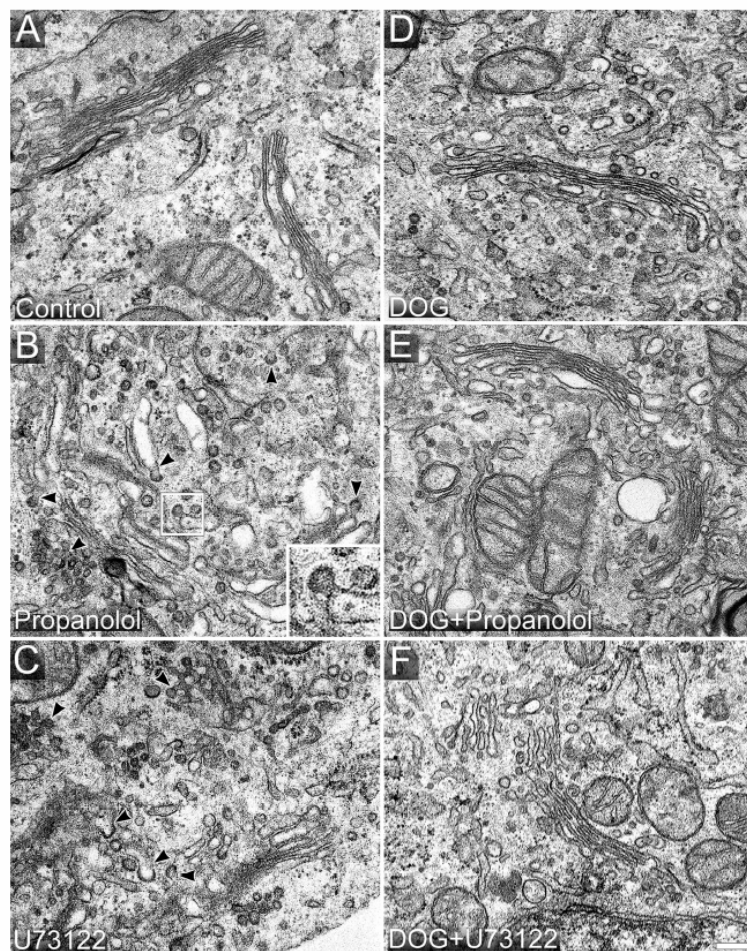
I. Fernández-Ulibarri *et al.*

Figure 8. Propanolol and U73122 induce a high density of COPI buds, which is counteracted by DOG and PDBu. Control (A), propanolol (60 μM; B)-, and U73122 (6 μM; C)-treated Vero cells were fixed and processed for conventional transmission electron microscopy (TEM). Normal Golgi stacks contained tightly attached 4–6 flat cisternae with a small number of peri-Golgi tubulovesicular profiles (A). Propanolol (B) and U73122 (C) treatments increased the number of peri-Golgi vesicular elements around swollen cisternae in the case of propanolol (B) or smaller cisternae in the case of U73122 (C). Both treatments induced vesicle-budding profiles containing an electron-dense coat that is characteristic of the COPI complex (arrowheads in B and C, and inset in B). Cells treated with DOG alone (3 μM; D) or pre-treated with DOG before propanolol (E) or U73122 (F) treatments showed a Golgi organization that was indistinguishable from control (A). Bar, 200 nm.

Video 7). Next, we tested whether DOG and PDBu prevented these Golgi ultrastructural alterations. Thus, DOG or PDBU were added 10 min before propanolol and, after 15 min of treatment, cells were processed for TEM. The Golgi ultrastructure in DOG plus propanolol- or U73122-treated cells (Figure 8E and F, respectively) was indistinguishable from that of control cells (Figure 8A). Similar results were obtained with PDBu (unpublished data). Importantly, neither DOG alone (Figure 8D) nor PDBu alone (unpublished data) produced any alteration in the Golgi organization. Stereological analysis (Table 1) indicates that propanolol increased the Golgi membrane surface area (as expected in a swelling process), whereas both propanolol and U73122 increased the density of peri-Golgi located round profiles. In contrast, there were no significant differences in any stereological parameter when control cells were compared with cells treated with DOG plus propanolol (Table 1). Overall, the ultrastructural analysis strongly suggests that propanolol and U73122 interfere with the fission process of Golgi-derived COPI-coated transport carriers resulting in an abnormally high number of Golgi-associated budding profiles. Moreover, this apparent arrest in membrane fission can be prevented by DOG and PDBu pretreatments.

The Decrease of the Golgi-associated DAG Pool Reduced ARFGAP1 But Not CtBP3/BARS in Golgi Membranes

Recent studies stress the importance of ARFGAP1 and CtBP3/BARS in COPI vesicle formation (Yang *et al.*, 2005). In an attempt to examine functional coupling between DAG and CtBP3/BARS, Vero cells were first treated with propanolol and then permeabilized with streptolysin O (SLO) to remove most of the nuclear and cytoplasmic pools of CtBP3/BARS and facilitate its detection at the Golgi (Supplementary Figure 7A). Neither propanolol (Supplementary Figure 7B) nor U73122 (unpublished data), nor both agents added together decreased the Golgi-associated CtBP3/BARS pool (Supplementary Figure 7C). Next, we tested the Golgi-localized protein ARFGAP1, which controls the formation of the COPI-coated transport carriers at the ER–Golgi interface (Yang *et al.*, 2002; Bigay *et al.*, 2003; Lee *et al.*, 2005) and whose activation seems to be partially dependent on DAGs (Antonny *et al.*, 1997). As expected, GFP-ARFGAP1 was almost exclusively seen in the Golgi (Figure 10A). The expression of GFP-ARFGAP1 did not alter the Golgi localization of either β-COP or CtBP3/BARS (unpublished data). We then monitored the dynamics of GFP-ARFGAP1 by in vivo

Figure 9. Electron tomography reveals that propanolol arrested COPI-coated transport carriers during fission from Golgi cisternae. Untreated (A) and propanolol (60 μM; B–D)-treated NRK cells were processed for TEM. As observed in Vero cells (Figure 8), propanolol induced cisternae swelling, and COP-coated vesicular profiles both closely localized and attached to cisternae. The latter is easily seen because of the formation of a narrow neck between the transport carrier and the cisterna (arrowheads). Two representative COPI-coated budding vesicles are shown in the inset. (C) Consecutive 6-nm-thick virtual slices extracted from the tomogram. (D) 3D modeling generated by manual segmenting of the tomographic data shown in C. Cisternae are shown in blue, COP-coated round profiles attached to cisternae in red and fully isolated vesicles in green. D2 panel is the same as D1, but it has been laterally rotated 45° about the X axis. D3 panel is an enlargement of a zone shown in the adjacent other two panels, to show a better view of the numerous vesicles attached (red) to the lateral rims of cisternae (blue). Original tomogram plus segmented contours together with the modeled data derived from the 3D reconstruction can be viewed in Supplementary Videos 7 and 8, respectively. Videos allow better visualization of the connections between COP-coated vesicles and cisternae in propanolol-treated cells. Bar, 200 nm.
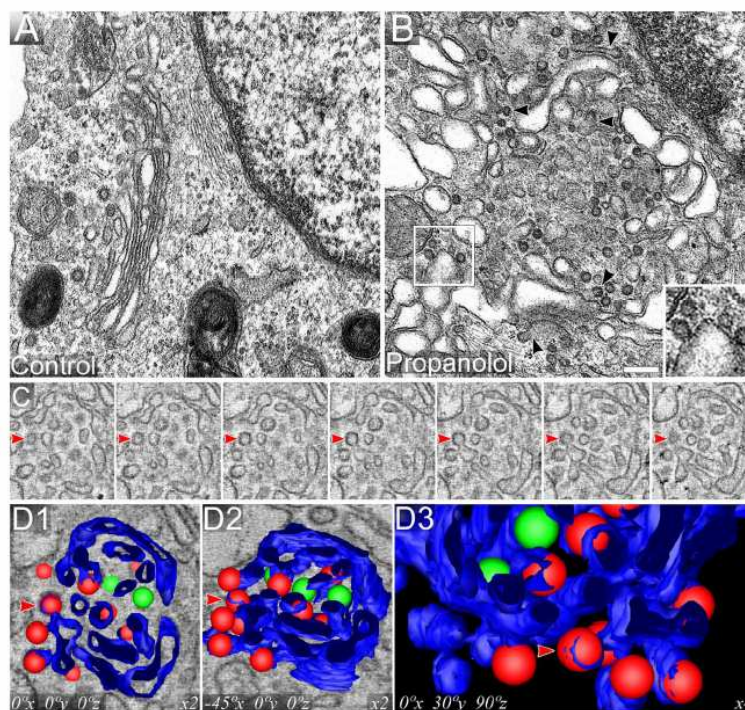
confocal microscopy. Propanolol reduced GFP-ARFGAP1 in the Golgi by ~50% (Figures 10, B and C; Supplementary Video 9). U73122 treatment led to a milder reduction (unpublished data). Pretreatment with DOG significantly offset this decrease (Figure 10, B and C; Supplementary Video 10). DOG alone did not alter the Golgi localization of GFP-ARFGAP1 (Figure 10, B and C). Therefore, data indicate that DAG directly participates in the functional recruitment of ARFGAP1 to the Golgi.

DISCUSSION

The current study shows that a decrease in DAG at the Golgi affects retrograde (Golgi-to-ER) but not anterograde (ER-to-Golgi) membrane transport. Reducing Golgi DAG decreases

the dynamic interaction of ARFGAP1 with Golgi membranes and causes a blockade in the formation of COPI-coated vesicles. Our experimental evidence is based on the use of propanolol and U73122, two compounds that are known to diminish cellular DAG content. We demonstrate that both drugs significantly reduce Golgi-associated DAG levels, and, in addition, that PKD-KD and the C1b-PKCθ domain (two established reporters for DAG) redistribute from the Golgi to the cytosol. It is important to note that propanolol and U73122 were used at relatively low concentrations (60 and 6 μM, respectively), lower than the usual concentrations used in pharmacological studies (Stiles *et al.*, 1984). Our conclusion that a decrease in DAG impairs retrograde transport is supported by the finding that both DOG and PDBU counteract the effects of propanolol and U73122 treatments.

Table 1. Stereological analysis of the Golgi complex in NRK cells

	V_{cist-G} (%)[a]	S_{cist-G} (μm^{-1})[b]	N_{ves-G} (μm^{-3})[c]	N_{bud} (n)[d]
Control	36.7 ± 2.3	16.0 ± 3.0	267.0 ± 33.3	1.1 ± 0.4
Propanolol	40.7 ± 3.0**[e]	20.2 ± 4.0*	592.8 ± 45.5***	4.0 ± 1.0***
U73122	38.2 ± 1.2	17.4 ± 1.5	496.3 ± 57.9***	3.0 ± 0.7***
DOG	37.1 ± 2.0	15.8 ± 1.2	286 ± 34	1.0 ± 0.6
DOG + propanolol	38.1 ± 3.3	17.1 ± 2.0	301 ± 40	1.3 ± 0.6
DOG + U73122	37.3 ± 2.7	16.1 ± 1.9	281 ± 62	1.1 ± 0.4

[a] V_{cist-G}, volume density.

[b] S_{cist-G}, surface density of cisternae.

[c] N_{ves-G}, numerical density of peri-Golgi vesicle profiles.

[d] N_{bud}, number of Golgi buds per μm^2.

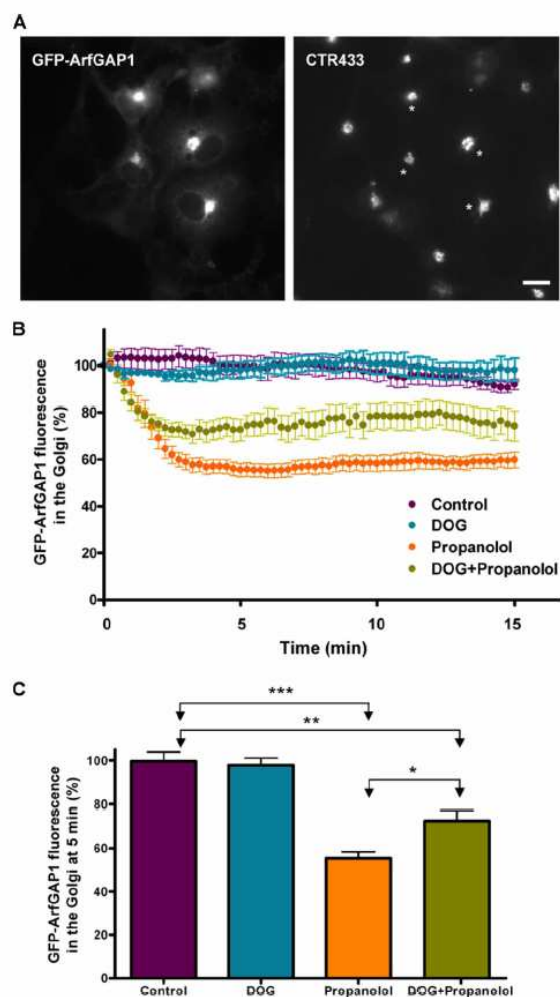[e] Statistical significance: *$p \leq 0.05$, **$p \leq 0.01$, ***$p \leq 0.001$.

I. Fernández-Ulibarri *et al.*

Figure 10. Propanolol decreased GFP-ARFGAP1 in the Golgi complex. COS-1 cells were transiently transfected with a plasmid coding for GFP-ARFGAP1, which colocalizes with the Golgi marker CTR433 (A; asterisks indicate transfected cells). (B) Golgi-associated GFP fluorescence measurement from ARFGAP1 of transfected cells after propanolol (60 μM) or DOG (3 μM) plus propanolol treatments. Propanolol lowered the amount of ARFGAP1 in the Golgi by ~50% for at least 30 min (Supplementary Video 9). DOG pretreatment significantly mitigated this reduction (Supplementary Video 10) and DOG alone did not affect the Golgi-associated fluorescence of ARFGAP1 (unpublished data). Bar, 10 μm. (C) Quantitative analysis of the Golgi-associated GFP-ARFGAP1 fluorescence measured in cells (n = 8) after 5 min of each treatment. Statistical significance, **p $\leq$ 0.01 and ***p $\leq$ 0.001.

DAG and Membrane Traffic at the ER–Golgi interface

Our results of the ER-to-Golgi VSV-G transport and the Golgi reassembly after the BFA washout indicate that the early anterograde (ER-to-Golgi) protein transport is not dependent on the DAG pool(s) decreased by propanolol, U73122, or FB1. Conversely, unlike FB1, both propanolol and U73122 impair retrograde (Golgi-to-ER) protein transport, as shown by the delay in the BFA-induced Golgi disassembly and by the consistent change in the subcellular distribution of the KDELr,

which led to a Golgi-like staining pattern. This is indicative that KDELr is retained in the Golgi. Importantly, DOG or PDBU, which are incorporated to the Golgi, prevented the propanolol/U73122-induced morphological alterations, which strongly indicates that such alterations were caused by the reduction of the Golgi-associated DAG pool(s). It is tempting to speculate that propanolol, U73122, and FB1 all reduce Golgi-associated DAG, but they probably affect different DAG pools, explaining why propanolol has more pronounced effects on Golgi-to-ER traffic than U73122, whereas FB1 reduces Golgi DAG without any measurable effect on Golgi-to-ER traffic. This hypothesis can also be extrapolated to late Golgi compartments because VSV-G post-Golgi transport is blocked by FB1 but not by U73122, suggesting that as at the ER–Golgi interface, different DAG pools participate in formation of TGN-derived transport carriers. Therefore, it would be very informative to find out whether transport carriers derived from different Golgi compartments (*cis*- and *trans*-TGN) are specifically associated with different molecular species of DAG. In turn, this could also determine the particular fission molecular machinery recruitment at each Golgi compartment required to generate specific transport carriers (see below). In any case, we cannot exclude other possibilities to explain the different membrane trafficking sensitivity to these agents such as that the same DAG species are present at several Golgi compartments but in different membrane contexts (for instance, different rate of cholesterol and/or other neighbor lipids) and/or that the targeted enzymes are merely localized in different Golgi compartments.

Role of DAG in the Fission of COPI Transport Carriers

Ultrastructural analysis of the Golgi architecture in propanolol/U73122-treated cells clearly shows the accumulation of COPI-coated vesicle profiles next to Golgi cisternae. Electron tomography and 3D modeling showed a preponderance of COPI-coated vesicle buds, which indicates that the decrease of Golgi-associated DAG levels caused by propanolol and U73122 impairs the membrane scission of COPI-coated transport carriers from the cisterna. The numerous budding profiles seen in treated cells are consistent with the postulated role of DAG as a lipid participating in neck formation in a Golgi-derived vesicle or tubule (Shemesh *et al.*, 2003), regardless whether originating from the TGN (Bard and Malhotra, 2006) or from an early Golgi compartment (our results here). This structural role is assigned on the basis of the fact that DAG has a much smaller head group than other lipids turning into a lipid with a pronounced cone shape. Consequently, DAG reduces the lipid head group packing and creates membrane insertion sites, allowing peripheral membrane proteins (such as ARFGAP1, see below) to access the central, hydrophobic portion of the bilayer, where they may subsequently trigger the generation of membrane curvature (Nie and Randazzo, 2006). Thus, a reduction in DAG levels of Golgi membranes would be expected to result in a more tightly packed membrane surface, and reduce the efficiency of, or even inactivate, the molecular machinery required to induce membrane fission. What may mark the difference between the TGN- and the early Golgi-derived transport carrier formation is the different type of DAG generated in each compartment and, consequently, the fission-associated molecular machinery recruited to each site. In accordance with this postulate, we could explain the different membrane trafficking results obtained using FB1 in the TGN (where it blocks post-Golgi protein transport; Baron and Malhotra, 2002) or at the ER–Golgi interface (no alteration; present results). The latter suggests that the DAG

3260

derived from the Golgi-localized SM synthase 1 (Huitema *et al.*, 2004) could only be involved in post-Golgi trafficking. On the other hand, the mechanical role of DAG may also be tightly associated with the recruitment and activation of membrane-deformation and fission-scaffold proteins involved in the COPI-coated transport carriers, as reported for noncoated carriers in the TGN (Bard and Malhotra, 2006). Thus, the induced decrease of Golgi-associated DAG pool triggers the cytosolic redistribution of a significant amount of the Golgi-associated ARFGAP1 pool, which in turn is crucial to coatomer assembly and the subsequent deformation of Golgi-derived transport carriers (Bigay *et al.*, 2003; Liu *et al.*, 2005). Note that despite the decrease of ARFGAP1 in the Golgi, the localization of coatomer (reported by β-COP) and CtBP3/BARS was unaltered. In accordance with the former, EM images show numerous buds fully covered with the characteristic COPI coat. This result is not surprising because although ARFGAP1 and CtBP3/BARS interact directly in the COPI coat, they are recruited to the Golgi independently (Yang *et al.*, 2005). Furthermore, pretreatment with DOG significantly mitigated the propanolol-induced release of ARFGAP1 from Golgi membranes in vivo. Therefore, our results indicate that DAG is required to recruit ARFGAP1 to early Golgi compartments and thus needed for the fission of COPI-coated transport carriers. Conversely, it is much less clear why the BFA-stimulated (COPI-independent) tubule-mediated retrograde trafficking was also inhibited by propanolol and U73122. Interestingly, very similar results were also obtained with phospholipase A_2 (PLA$_2$) antagonists (Figueiredo *et al.*, 1999). However, we can only speculate that similar lipid-dependent changes in membrane curvature could be generated by DAG and PLA$_2$-derived lipids to explain tubule formation at the Golgi.

Finally, DAG may also be involved in membrane fusion events at the ER–Golgi interface. In this respect, we emphasize the continuous but erratic back-and-forth movement of abnormal BFA-induced Golgi-derived tubules in propanolol- and U73122-treated cells (at least in those cells that showed BFA-induced tubulation). This observation suggested, first, that BFA-induced tubules in propanolol/U73122-treated cells were abnormally formed, but the delay in the Golgi disassembly could also be attributable to defective fusion of these tubules with ER membranes. However, the finding that the Golgi was normally disassembled when propanolol or U73122 was added after BFA suggests that the primary cause was not defective membrane fusion. If that were the case, the Golgi disassembly should be equally affected regardless of whether propanolol or U73122 was added before, after, or at the same time as BFA.

In summary, our data indicate that DAG is required for the formation of COPI transport carriers at early Golgi compartments because it facilitates the recruitment of ARFGAP1. In addition, the results also suggest that different DAG moieties could be determinant in the specific recruitment of protein complexes directly responsible for sorting and/or membrane fission events in different Golgi compartments.

ACKNOWLEDGMENTS

REFERENCES

Alonso, R., Rodriguez, M. C., Pindado, J., Merino, E., Merida, I., and Izquierdo, M. (2005). Diacylglycerol kinase alpha regulates the secretion of lethal exosomes bearing Fas ligand during activation-induced cell death of T lymphocytes J. Biol. Chem. *280*, 28439–28450.

Antonny, B., Huber, I., Paris, S., Chabre, M., and Cassel, D. (1997). Activation of ADP-ribosylation factor 1 GTPase-activating protein by phosphatidylcholine-derived diacylglycerols. J. Biol. Chem. *272*, 30848–30851.

Balch, W. E., Dunphy, W. G., Braell, W. A., and Rothman, J. E. (1984). Reconstitution of the transport of protein between successive compartments of the Golgi measured by the coupled incorporation of N-acetylglucosamine. Cell *39*, 405–416.

Bankaitis, V. A., Aitken, J. R., Cleves, A. E., and Dowhan, W. (1990). An essential role for a phospholipid transfer protein in yeast Golgi function. Nature *347*, 561–562.

Bard, F., and Malhotra, V. (2006). The formation of TGN-to-plasma-membrane transport carriers. Annu. Rev. Cell Dev. Biol. *22*, 439–455.

Baron, C. L., and Malhotra, V. (2002). Role of diacylglycerol in PKD recruitment to the TGN and protein transport to the plasma membrane. Science *295*, 325–328.

Bigay, J., Casella, J. F., Drin, G., Mesmin, B., and Antonny, B. (2005). ArfGAP1 responds to membrane curvature through the folding of a lipid packing sensor motif. EMBO J. *24*, 2244–2253.

Bigay, J., Gounon, P., Robineau, S., and Antonny, B. (2003). Lipid packing sensed by ArfGAP1 couples COPI coat disassembly to membrane bilayer curvature. Nature *426*, 563–566.

Bleasdale, J. E., Thakur, N. R., Gremban, R. S., Bundy, G. L., Fitzpatrick, F. A., Smith, R. J., and Bunting, S. (1990). Selective inhibition of receptor-coupled phospholipase C-dependent processes in human platelets and polymorphonuclear neutrophils. J. Pharmacol. Exp. Ther. *255*, 756–768.

Bligh, E. G., and Dyer, W. J. (1959). A rapid method of total lipid extraction and purification. Can. J. Biochem. Physiol. *37*, 911–917.

Bonazzi, M. et al. (2005). CtBP3/BARS drives membrane fission in dynamin-independent transport pathways. Nat. Cell Biol. *7*, 570–580.

Caloca, M. J., Zugaza, J. L., and Bustelo, X. R. (2003). Exchange factors of the RasGRP family mediate Ras activation in the Golgi. J. Biol. Chem. *278*, 33465–33473.

Carrasco, S., and Mérida, I. (2004). Diacylglycerol-dependent binding recruits PKCtheta and RasGRP1 C1 domains to specific subcellular localizations in living T lymphocytes. Mol. Biol. Cell *15*, 2932–2942.

Chen, Y. G., Siddhanta, A., Austin, C. D., Hammond, S. M., Sung, T. C., Frohman, M. A., Morris, A. J., and Shields, D. (1997). Phospholipase D stimulates release of nascent secretory vesicles from the trans-Golgi network. J. Cell Biol. *138*, 495–504.

Chernomordik, L., Kozlov, M. M., and Zimmerberg, J. (1995). Lipids in biological membrane fusion. J. Membr. Biol. *146*, 1–14.

Claro, E., Sarri, E., and Picatoste, F. (1993). Endogenous phosphoinositide precursors of inositol phosphates in rat brain cortical membranes. Biochem. Biophys. Res. Commun. *193*, 1061–1067.

Colón-González, F., and Kazanietz, M. G. (2006). C1 domains exposed: from diacylglycerol binding to protein-protein interactions. Biochim. Biophys. Acta *1761*, 827–837.

Corda, D., Colanzi, A., and Luini, A. (2006). The multiple activities of CtBP/BARS proteins: the Golgi view. Trends Cell Biol. *16*, 167–173.

De Matteis, M. A., and Godi, A. (2004). Protein-lipid interactions in membrane trafficking at the Golgi complex. Biochim. Biophys. Acta *1666*, 264–274.

Díaz Anel, A. M., and Malhotra, V. (2005). PKCeta is required for beta1gamma2/beta3gamma2- and PKD-mediated transport to the cell surface and the organization of the Golgi apparatus. Cell Biol. *169*, 83–891.

Egea, G., Lázaro-Diéguez, F., and Vilella, M. (2006). Actin dynamics at the Golgi complex in mammalian cells. Curr. Opin. Cell Biol. *18*, 168–178.

Exton, J. H. (1994). Phosphatidylcholine breakdown and signal transduction. Biochim. Biophys. Acta *1212*, 26–42.

Freyberg, Z., Siddhanta, A., and Shields, D. (2003). "Slip, sliding away": phospholipase D and the Golgi apparatus. Trends Cell Biol. *13*, 540–546.

Figueiredo P. de, Polizotto, R. S., Drecktrah, D., and Brown, W. J. (1999). Membrane tubule-mediated reassembly and maintenance of the Golgi complex is disrupted by phospholipase A_2 antagonists. Mol. Biol. Cell *10*, 1763–1782.

I. Fernández-Ulibarri *et al.*

Freyberg, Z., Sweeney, D., Siddhanta, A., Bourgoin, S., Frohman, M., and Shields, D. (2001). Intracellular localization of phospholipase D1 in mammalian cells. Mol. Biol. Cell *12*, 943–955.

Freyberg, Z., Bourgoin, S., and Shields, D. (2002). Phospholipase D2 is localized to the rims of the Golgi apparatus in mammalian cells. Mol. Biol. Cell *13*, 3930–3942.

Gallop, J. L., Butler, P. J., and McMahon, H. T. (2005). Endophilin and CtBP/BARS are not acyltransferases in endocytosis or Golgi fission. Nature *438*, 675–678.

Goñi, F. M., and Alonso, A. (1999). Structure and functional properties of diacylglycerols in membranes. Prog. Lipid Res. *38*, 1–48.

Hausser, A., Storz, P., Martens, S., Link, G., Toker, A., and Pfizenmaier, K. (2005). Protein kinase D regulates vesicular transport by phosphorylating and activating phosphatidylinositol-4 kinase IIIbeta at the Golgi complex. Nat. Cell Biol. *7*, 880–886.

Holthuis, J. C., and Burger, K. N. (2003). Sensing membrane curvature. Dev. Cell *5*, 821–822.

Huijbregts, R. P., Topalof, L., and Bankaitis, V. A. (2000). Lipid metabolism and regulation of membrane trafficking. Traffic *1*, 195–202.

Huitema, K., van den Dikkenberg, J., Brouwers, J. F., and Holthuis, J. C. (2004). Identification of a family of animal sphingomyelin synthases. EMBO J. *23*, 33–44.

Ichikawa, S., and Hirabayashi, Y. (1998). Glucosylceramide synthase and glycosphingolipid synthesis. Trends Cell Biol. *8*, 198–202.

Jun, Y., Fratti, R. A., and Wickner, W. (2004). Diacylglycerol and its formation by phospholipase C regulate Rab- and SNARE-dependent yeast vacuole fusion. J. Biol. Chem. *279*, 53186–53195.

Kearns, B. G., McGee, T. P., Mayinger, P., Gedvilaite, A., Phillips, S. E., Kagiwada, S., and Bankaitis, V. A. (1997). Essential role for diacylglycerol in protein transport from the yeast Golgi complex. Nature. *387*, 101–105.

Klausner, R. D., Donaldson, J. G., and Lippincott-Schwartz, J. (1992). Brefeldin A: insights into the control of membrane traffic and organelle structure. J. Cell Biol. *116*, 1071–1080.

Kooijman, E. E., Chupin, V., de Kruijff, B., and Burger, K. N. (2003). Modulation of membrane curvature by phosphatidic acid and lysophosphatidic acid. Traffic *4*, 162–174.

Kooijman, E. E., Tieleman, D. P., Testerink, C., Munnik, T., Rijkers, D. T., Burger, K.N., and de Kruijff, B. (2007). An electrostatic/hydrogen bond switch as basis for the specific interaction of phosphatidic acid with proteins. J. Biol. Chem. *282*, 11356–11364.

Kremer, J. R., Mastronarde, D. N., and McIntosh, J. R. (1996). Computer visualization of three-dimensional image data using IMOD. J. Struct. Biol. *116*, 71–76.

Lee, C. S., Kim, I. S., Park, J. B., Lee, M. N., Lee, H. Y., Suh, P. G., and Ryu, S. H. (2006). The phox homology domain of phospholipase D activates dynamin GTPase activity and accelerates EGFR endocytosis. Nat. Cell Biol. *8*, 477–484.

Lee, S. Y., Yang, J. S., Hong, W., Premont, R. T., and Hsu, V. W. (2005). ARFGAP1 plays a central role in coupling COPI cargo sorting with vesicle formation. J. Cell Biol. *168*, 281–290.

Lehel, C., Olah, Z., Jakab, G., Szallasi, Z., Petrovics, G., Harta, G., Blumberg, P. M., and Anderson, W. B. (1995). Protein kinase C epsilon subcellular localization domains and proteolytic degradation sites. A model for protein kinase C conformational changes. J. Biol. Chem. *270*, 19651–19658.

Leikin, S., Kozlov, M. M., Fuller, N. L., and Rand, R. P. (1996). Measured effects of diacylglycerol on structural and elastic properties of phospholipid membranes. Biophys. J. *71*, 2623–2632.

Lewis, M. J., and Pelham, H. R. (1992). Ligand-induced redistribution of a human KDEL receptor from the Golgi complex to the endoplasmic reticulum. Cell *68*, 353–364.

Liljedahl, M., Maeda, Y., Colanzi, A., Ayala, I., Van Lint, J., and Malhotra, V. (2001). Protein kinase D regulates the fission of cell surface destined transport carriers from the trans-Golgi network Cell *104*, 409–420.

Liu, W., Duden, R., Phair, R. D., and Lippincott-Schwartz, J. (2005). ArfGAP1 dynamics and its role in COPI coat assembly on Golgi membranes of living cells. J. Cell Biol. *168*, 1053–1063.

Litvak V., Dahan N., Ramachandran S., Sabanay H., and Lev, S. (2005). Maintenance of the diacylglycerol level in the Golgi apparatus by the Nir2 protein is critical for Golgi secretory function. Nat. Cell Biol. *7*, 225–234 (Erratum in: Nat. Cell Biol. 2005 *7*, 431).

Luberto, C., and Hannun, Y. A. (1998). Sphingomyelin synthase, a potential regulator of intracellular levels of ceramide and diacylglycerol during SV40

transformation. Does sphingomyelin synthase account for the putative phosphatidylcholine-specific phospholipase C. J. Biol. Chem. *273*, 14550–14559.

Maeda, Y., Beznoussenko, G. V., Van Lint, J., Mironov, A. A., and Malhotra, V. (2001). Recruitment of protein kinase D to the trans-Golgi network via the first cysteine-rich domain. EMBO J. *20*, 5982–5990.

Maissel, A., Marom, M., Shtutman, M., Shahaf, G., and Livneh, E. (2006). PKCeta is localized in the Golgi, ER and nuclear envelope and translocates to the nuclear envelope upon PMA activation and serum-starvation: C1b domain and the pseudosubstrate containing fragment target PKCeta to the Golgi and the nuclear envelope. Cell Signal. *18*, 1127–1139.

Mastronade, N. D. (1997). Dual-axis tomography: an approach with alignment methods that preserve resolution. J. Struct. Biol. *120*, 343–352.

Merrill, A. H. Jr., Sullards, M. C., Wang, E., Voss, K. A., and Riley, R. T. (2001). Sphingolipid metabolism: roles in signal transduction and disruption by fumonisins. Environ. Health Perspect. *2*, 283–289.

Mesmin, B., Drin, G., Levi, S., Rawet, M., Cassel, D., Bigay, J., and Antonny, B. (2007). Two lipid-packing sensor motifs contribute to the sensitivity of ArfGAP1 to membrane curvature. Biochemistry *46*, 1779–1790.

Murshid, A., and Presley, J. F. (2004). ER-to-Golgi transport and cytoskeletal interactions in animal cells. Cell Mol. Life Sci. *61*, 133–145.

Nagaya, H., Wada, I., Jia, Y. J., and Kanoh, H. (2002). Diacylglycerol kinase delta suppresses ER-to-Golgi traffic via its SAM and PH domains. Mol. Biol. Cell *13*, 302–316.

Nie, Z., and Randazzo, P. A. (2006). Arf GAPs and membrane traffic. J. Cell Sci. *119*, 1203–1211.

Pappu, A. S., and Hauser, G. (1983). Propranolol-induced inhibition of rat brain cytoplasmic phosphatidate phosphohydrolase. Neurochem. Res. *8*, 1565–1575.

Pathre, P., Shome, K., Blumental-Perry, A., Bielli, A., Haney, C. J., Alber, S., Watkins, S. C., Romero, G., and Aridor, M. (2003). Activation of phospholipase D by the small GTPase Sar1p is required to support COPII assembly and ER export. EMBO J. *22*, 4059–4069.

Preiss, J. E., Loomis, C. R., Bell, R. M., and Niedel, J. E. (1987). Quantitative measurement of sn-1,2-diacylglycerols. Methods Enzymol. *141*, 294–300.

Prestle, J., Pfizenmaier, K., Brenner, J., and Johannes, F. J. (1996). Protein kinase C mu is located at the Golgi compartment. J. Cell Biol. *134*, 1401–1410.

Quest, A. F., Bardes, E. S., and Bell, R. M. (1994). A phorbol ester binding domain of protein kinase C gamma. High affinity binding to a glutathione-S-transferase/Cys2 fusion protein. J. Biol. Chem. *269*, 2953–2960.

Rhee, S. G. (2001). Regulation of phosphoinositide-specific phospholipase C. Annu. Rev. Biochem. *70*, 281–312.

Roberts, R., Sciorra, V. A., and Morris, A. J. (1998). Human type 2 phosphatidic acid phosphohydrolases. Substrate specificity of the type 2a, 2b, and 2c enzymes and cell surface activity of the 2a isoform. J. Biol. Chem. *273*, 22059–22067.

Roth, M. G., Bi, K., Ktistakis, N. T., and Yu, S. (1999). Phospholipase D as an effector for ADP-ribosylation factor in the regulation of vesicular traffic. Chem. Phys. Lipids *98*, 141–152.

Satoh, T., Edamatsu, H., and Kataoka, T. (2005). Phospholipase cepsilon guanine nucleotide exchange factor activity and activation of rap1. Methods Enzymol. *407*, 281–290.

Schutze, S., Potthoff, K., Machleidt, T., Berkovic, D., Wiegmann, K., and Kronke, M. (1992). TNF activates NF-kappa B by phosphatidylcholine-specific phospholipase C-induced "acidic" sphingomyelin breakdown Cell *71*, 765–776.

Sciaky, N., Presley, J., Smith, C., Zaal, K. J., Cole, N., Moreira, J. E., Terasaki, M., Siggia, E., and Lippincott-Schwartz, J. (1997). Golgi tubule traffic and the effects of brefeldin A visualized in living cells. J. Cell Biol. *139*, 1137–1155.

Sciorra, V. A., and Morris, A. J. (1999). Sequential actions of phospholipase D and phosphatidic acid phosphohydrolase 2b generate diglyceride in mammalian cells. Mol. Biol. Cell *10*, 3863–3876.

Shemesh, T., Luini, A., Malhotra, V., Burger, K. N., and Kozlov, M. M. (2003). Prefission constriction of Golgi tubular carriers driven by local lipid metabolism: a theoretical model. Biophys. J. *85*, 3813–3827.

Siddhanta, A., and Shields, D. (1998). Secretory vesicle budding from the trans-Golgi network is mediated by phosphatidic acid levels. J. Biol. Chem. *273*, 17995–17998.

Speight, P., and Silverman, M. (2005). Diacylglycerol-activated Hmunc13 serves as an effector of the GTPase Rab34. Traffic *6*, 858–865.

Stiles, G. L., Caron, M. G., and Lefkowitz, R. J. (1984). Beta-adrenergic receptors: biochemical mechanisms of physiological regulation. Physiol. Rev. *64*, 661–743.

Thompson, A. K., Mostafapour, S. P., Denlinger, L. C., Bleasdale, J. E., and Fisher, S. K. (1991). The aminosteroid U-73122 inhibits muscarinic receptor sequestration and phosphoinositide hydrolysis in SK-N-SH neuroblastoma cells. A role for Gp in receptor compartmentation. J. Biol. Chem. *266*, 23856–23862.

Tuscher, O., Lorra, C., Bouma, B., Wirtz, K. W., and Huttner, W. B. (1997). Cooperativity of phosphatidylinositol transfer protein and phospholipase D in secretory vesicle formation from the TGN—phosphoinositides as a common denominator? FEBS Lett. *419*, 271–275.

Valderrama, F., Babia, T., Ayala, I., Kok, J. W., Renau-Piqueras, J., and Egea, G. (1998). Actin microfilaments are essential for the cytological positioning and morphology of the Golgi complex. Eur. J. Cell Biol. *76*, 9–17.

Wang, E., Norred, W. P., Bacon, C. W., Riley, R. T., and Merrill, A. H., Jr. (1991). Inhibition of sphingolipid biosynthesis by fumonisins. Implications for diseases associated with *Fusarium moniliforme*. J. Biol. Chem. *266*, 14486–14490.

Wang, Q. J., Bhattacharyya, D., Garfield, S., Nacro, K., Marquez, V. E., and Blumberg, P. M. (1999). Differential localization of protein kinase C delta by phorbol esters and related compounds using a fusion protein with green fluorescent protein. J. Biol. Chem. *274*, 37233–37239.

Wang, Y. J., Wang, J., Sun, H. Q., Martinez, M., Sun, Y. X., Macia, E., Kirchhausen, T., Albanesi, J. P., Roth, M. G., and Yin, H. L. (2003). Phosphatidylinositol 4 phosphate regulates targeting of clathrin adaptor AP-1 complexes to the Golgi. Cell *114*, 299–310.

Weigert, R. *et al.* (1999). CtBP/BARS induces fission of Golgi membranes by acylating lysophosphatidic acid. Nature *402*, 429–433.

Weixel, K. M., Blumental-Perry, A., Watkins, S. C., Aridor, M., and Weisz, O. A. (2005). Distinct Golgi populations of phosphatidylinositol 4-phosphate regulated by phosphatidylinositol 4-kinases. J. Biol. Chem. *280*, 10501–10508.

Wu, W. I., McDonough, V. M., Nickels, J. T., Jr., Ko, J., Fischl, A. S., Vales, T. R., Merrill, A. H., Jr., and Carman, G. M. (1995). Regulation of lipid biosynthesis in *Saccharomyces cerevisiae* by fumonisin B1. J. Biol. Chem. *270*, 13171–13178.

Yang, J. S., Lee, S. Y., Spano, S., Gad, H., Zhang, L., Nie, Z., Bonazzi, M., Corda, D., Luini, A., and Hsu, V. W. (2005). A role for BARS at the fission step of COPI vesicle formation from Golgi membrane. EMBO J. *24*, 4133–4143.

Yang, J. S., Lee, S. Y., Gao, M., Bourgoin, S., Randazzo, P. A., Premont, R. T., and Hsu, V. W. (2002). ARFGAP1 promotes the formation of COPI vesicles, suggesting function as a component of the coat. J. Cell Biol. *159*, 69–78.

Yeaman, C., Ayala, M. I., Wright, J. R., Bard, F., Bossard, C., Ang, A., Maeda, Y., Seufferlein, T., Mellman, I., Nelson, W. J., and Malhotra, V. (2004). Protein kinase D regulates basolateral membrane protein exit from trans-Golgi network. Nat. Cell Biol. *6*, 106–112.

Ziese, U., Janssen, A. H., Murk, J. L., Geerts, W. J., Van der Krift, T., Verkleij, A. J., and Koster, A. J. (2002). Automated high-throughput electron tomography by pre-calibration of image shifts. J. Microsc. *205*, 187–200.